J. Phys. B: At. Mol. Opt. Phys. **22** (1989) 3001-3009. Printed in the UK

The NVV Auger electron spectrum of the HI molecule

Leif Karlsson, Svante Svensson, Peter Baltzer, Mats Carlsson-Göthe, Michael P Keane, Arnaldo Naves de Brito, Nestor Correia and Björn Wannberg

Department of Physics, University of Uppsala, PO Box 530, S-75121 Uppsala, Sweden

Received 25 May 1989

Abstract. The electron-beam-excited NVV Auger electron spectrum of HI is presented together with a new recording of the x-ray excited photoelectron spectrum of the I 4d core lines. It is shown that the initial I 4d core hole state is vibrationally excited. The NVV Auger electron spectrum is dominated by transitions to the π^{-2} dicationic states of $^3\Sigma^-$, $^1\Delta$ and $^1\Sigma^+$ symmetry. Vibrational structure is resolved in all Auger transitions and the equilibrium geometry of both the initial core-hole state and the final dicationic states have been determined. A splitting of the $^3\Sigma_1^-$ and $^3\Sigma_0^-$ states of 220 meV is observed. The dissociation of the π^{-2} dicationic states in terms of Coulomb explosion is discussed and tentative potential curves are given.

1. Introduction

In recent studies, using electron-beam-excited Auger electron spectroscopy, we have shown the existence of quasi-stable states in the doubly ionised HCl/DCl (Karlsson *et al* 1988, Svensson *et al* 1989) and HBr/DBr (Wannberg *et al* 1989) molecules. These quasi-stable states are all formed within the $1\pi^{-2}$ valence electron configuration and are of $^3\Sigma^-$, $^1\Delta$ and $^1\Sigma^+$ symmetry. The potential curves for these states could be studied due to resolution of vibrational fine structure in the Auger electron bands corresponding to the $L \rightarrow 1\pi^{-2}$ and $M \rightarrow 1\pi^{-2}$ transitions in HCl/DCl and HBr/DBr, respectively. By a Franck-Condon analysis and using Morse curves we could sketch the form of the potential curves near the equilibrium. For large internuclear distances the dissociation proceeds via the well known Coulomb explosion mechanism, i.e. the dication separates into singly ionised fragments. By combining the Morse curves and the Coulomb potential curves it was possible to determine the tunnelling barrier form of the potential for the quasi-stable states.

The Coulomb explosion mechanism for the dissociation of these doubly ionised states has been verified by measurements of the kinetic energies of the proton fragments (Baltzer *et al* 1988b). These measurements were carried out using the same electron spectrometer that was used for the Auger measurements. The only change that was made was a reversal of the relevant voltages (Baltzer *et al* 1988a).

The Auger electron spectra corresponding to the $L \rightarrow 1\pi^{-2}$ and $M \rightarrow 1\pi^{-2}$ transitions in HCl/DCl and HBr/DBr, respectively, are very similar and show essentially four bands representing six different Auger transitions. Looking closer at the finer details of the structures the overlapping bands could be identified and an assignment could be made. This assignment could be performed in terms of pure $\Lambda\Sigma$ coupling of the final states. This is in accordance with the Auger electron spectra from Ar and Kr

0953-4075/89/193001+09$02.50

(Werme *et al* 1972) where no appreciable splitting between the $^3P_{0,1}$ components is observed. It is therefore not necessary to include intermediate coupling in the theoretical description of these components.

In the doubly ionised states of Xe, however, intermediate coupling is important for the theoretical description of the Auger electron spectrum. The splitting between the $^3P_{0,1}$ components in the NOO Auger electron spectrum is as large as 220 meV (Werme *et al* 1972). Thus one would expect that the intermediate coupling is also important in the case of the outermost doubly ionised states of HI. In this work we present the high resolution NVV Auger electron spectrum of HI and it is shown that this spectrum is more complex than the corresponding LVV and MVV Auger electron spectra from HCl and HBr, respectively. It is found that in order to explain this spectrum one has to consider several effects; the spin–orbit splittings of the initial 4d core-hole states, the vibrational structure of the initial and final states and in addition intermediate coupling.

2. Experimental method

The HI gas was commercially obtained. The purity of the gas was checked by ultraviolet photoelectron spectroscopy. Small amounts (<5%) of N_2, HCl and HBr were found in the sample. These impurities, however, do not give rise to lines in the Auger electron spectrum in the kinetic energy range 24–32 eV studied in this paper.

The Auger electron spectra were recorded on an electron spectrometer which has recently been redesigned to operate as a dedicated high-resolution instrument for gas phase studies using electron beam or UV excitation (Baltzer *et al* 1988a). For the present Auger electron studies an electron beam of 2 kV energy was used to create the initial I 4d core hole state. The pressure in the sample compartment was held below 1 Pa (a few mTorr). Several runs were made to check for instabilities in the electron gun and small pressure variations in the sample compartment. Calibration was made by mixing the sample gas with He and simultaneously recording the NVV Auger electron spectrum from HI along with the well known autoionisation spectrum of He. The (sp, 22) $(^1P) \rightarrow 1s(^2S_{1/2})$ transition with an energy 35.55 eV was used as the standard line.

In order to determine the double ionisation energies and to, at least qualitatively, establish the geometry of the initial core hole state a recording was made of the $4d_{3/2,5/2}$ photoelectron spectrum of HI where monochromatised x-rays ($h\nu = 1487$ eV) were used as excitation. These studies were carried out on a second photoelectron spectrometer at Uppsala, which is normally used for high-energy excitation. The x-ray photoelectron spectrum was calibrated by running the total 4d-valence spectrum between 0 and 60 eV binding energy. The outermost photoelectron line at 10.38 eV was used to calibrate the energy scale. This energy was in turn obtained by calibrating against the He line at 24.587 eV that is present in the He II excited photoelectron spectrum.

3. Results and discussion

The NVV Auger spectrum from the HI molecule appears at a low kinetic energy. In this energy range there is a high background intensity due to low-energy secondary electrons. This background completely dominates the spectrum below 20 eV and

therefore structures arising from the σ^{-2} and $\sigma^{-1}\pi^{-1}$ final-state configurations have not been detected in any detail. We therefore concentrate upon the assignment of the outermost part of the spectrum from 24–32 eV kinetic energy, corresponding essentially to transitions to states in the π^{-2} final configuration.

3.1. The 4d photoelectron spectrum

Before analysing the Auger electron spectrum it is necessary to discuss the x-ray excited photoelectron spectrum of the I 4d levels in HI. Upon Cl 2p core ionisation of HCl we have earlier shown (Svensson *et al* 1989), from the intensity of the $2p_{3/2}$ $(v=1)\rightarrow$ $\pi^{-2}\,{}^3\Sigma^-$ $(v=0)$ transition, that the core-hole state has an equilibrium distance of about 0.03 Å greater than the neutral ground state. For the Br 3d core ionisation the corresponding geometry change is found to be 0.12 Å (Wannberg *et al* 1989). In order to study the vibrational excitations in the I 4d core ionised state we have recorded the photoelectron spectrum shown in figure 1. The binding energies of the I $4d_{5/2}$ and the I $4d_{3/2}$ lines are 57.49 and 59.25 eV, respectively. Thus the spin-orbit splitting of the I 4d level is measured to be 1.76 eV. The figure reveals some other interesting details. The intensity ratio between the I $4d_{5/2}$ and the I $4d_{3/2}$ lines is 1.40 ± 0.05 which is somewhat smaller than the expected statistical ratio of 1.5. The width of the two lines is 0.69 ± 0.03 eV. This is substantially larger than the instrumental resolution, as obtained from a simultaneous recording of the outermost $1\pi_{3/2}$ line, which had a width of only 0.35 eV. The lifetime broadening is smaller than 0.1 eV (Keski-Rahkonen and

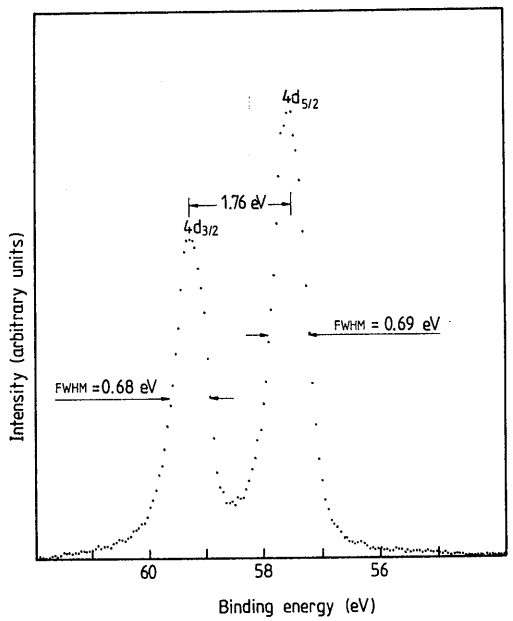

Figure 1. The photoelectron spectrum of the I 4d levels in HI excited by monochromatised x-rays ($h\nu=1487$ eV). The binding energies of the I $4d_{5/2}$ and I $4d_{3/2}$ lines are 57.49 and 59.25 eV. The spin-orbit splitting is thus observed to be 1.76 eV and the FWHM of the lines is 0.69 ± 0.03 eV. This FWHM is much larger than the FWHM of the outermost $1\pi_{3/2}$ level that was simultaneously recorded to be 0.35 eV. The line is thus vibrationally broadened, indicating a large change in the equilibrium geometry of the I 4d core-hole states when compared with the neutral ground state.

Krause 1974) and does not contribute appreciably to the measured width. Therefore we conclude that the I 4d lines are vibrationally broadened. Since the core-hole equilibrium bond distance should be larger than the equilibrium bond distance of the neutral ground state (1.160 916 Å, Huber and Herzberg 1979), we expect that the core hole vibrational energy should be somewhat smaller than the vibrational energy of the neutral ground state which is 286 meV (Huber and Herzberg 1979). The observed widths could therefore be explained by two strong vibrational components of approximately the same intensity followed by a progression of weaker vibrational lines at higher binding energies. These findings are also supported by the threshold photoelectron spectrum published by Morin and Nenner (1987) which shows two broad lines corresponding to photoionisation from the I 4d levels.

Using the harmonic approximation and simulating a lineshape by a Franck–Condon analysis and using an equilibrium distance of 1.78 ± 0.04 Å and vibrational energies in the region between 250–280 meV we obtain the observed spectrum. This reflects a large change in the equilibrium bond distance when compared with the neutral ground state, which may be associated with the spatial properties of the 4d electrons. This large change also fits with the trend observed for HCl and HBr.

3.2. Assignment of the NVV Auger electron spectrum

In figure 2 we show the NVV Auger electron spectrum between 23–32 eV kinetic energy. As many as 16 clearly observable structures and lines can be seen which are numbered in order of decreasing kinetic energy. These structures are grouped into five more or less distinct bands. The kinetic energies of these structures are given in table 1. It is clear from figure 2 that this spectrum is more complicated than the corresponding LVV and MVV spectra from HCl (Svensson *et al* 1989) and HBr (Wannberg *et al* 1989), respectively. The general features of the spectrum are, however, rather similar to the corresponding spectra from HCl and HBr, which facilitates in the interpretation of the present spectrum. Thus we might extrapolate from the HCl and HBr spectra to obtain the probable transition energies in the case of HI.

The first band at approximately 30 eV kinetic energy consists of the three lines labelled 1, 2 and 3. By comparison with the HCl and HBr spectra we expect that the $4d_{3/2} \rightarrow \pi^{-2}\,{}^3\Sigma^-$ transition gives rise to this band. In analogy to the earlier results we assign the strongest line, numbered 2, as the adiabatic $4d_{3/2}\ (v=0) \rightarrow \pi^{-2}\,{}^3\Sigma_1^-\ (v=0)$ transition. (For the moment we will postpone discussion of the $\Omega = 0$ component which would fall at approximately the same position as a possible $4d_{3/2}\ (v=1) \rightarrow \pi^{-2}\,{}^3\Sigma_1^-\ (v=0)$ transition, i.e. under 1.) Obviously line 3 then corresponds to the $4d_{3/2}\ (v=0) \rightarrow \pi^{-2}\,{}^3\Sigma_1^-\ (v=1)$ transition. The 0–1 vibrational spacing in the $\pi^{-2}\,{}^3\Sigma_1^-$ state is thus 220 meV as seen from table 1. This splitting is smaller than for the neutral ground state and corresponds to the general trend in relative decrease for the $\pi^{-2}\,{}^3\Sigma_1^-$ state vibrational energies when compared with the neutral ground state. For HCl a change of 48% (Svensson *et al* 1989, Morin and Nenner 1987) is observed while we find 35% for HBr (Wannberg *et al* 1989, Morin and Nenner 1987) and 23% for HI.

In order to make further assignments we have extrapolated the energy of the $4d_{3/2}\ (v=0) \rightarrow \pi^{-2}\,{}^1\Delta_2\ (v=0)$ transition from the known corresponding transitions in HCl and HBr. By correlating the $\pi^{-2}\,{}^1\Delta_2\ (v=0)$ energies to the first ionisation potentials we find that the $4d_{3/2}\ (v=0) \rightarrow \pi^{-2}\,{}^1\Delta_2\ (v=0)$ transition should fall at approximately 29.0 eV kinetic energy. This fits with peak 4 at 28.97 eV in the second group of lines. We therefore assign this line to the $4d_{3/2}\ (v=0) \rightarrow \pi^{-2}\,{}^1\Delta_2\ (v=0)$ transition and the

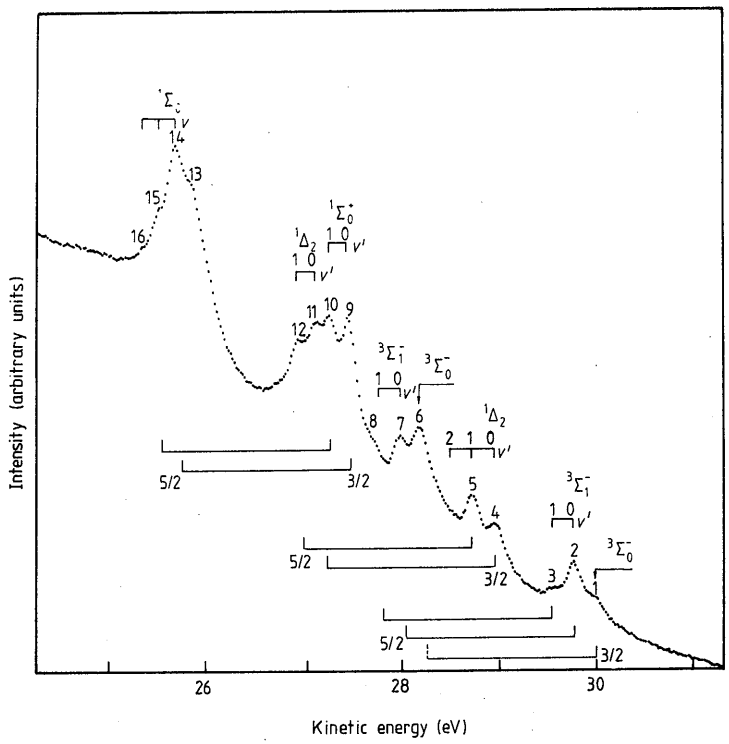

Figure 2. The NVV Auger electron spectrum of HI. A background of 46% of the intensity of the left-hand side of the spectrum is subtracted. This high background is due to the low kinetic energy in the spectrum. The NVV Auger spectrum of HI is more complicated than the corresponding LVV and MVV spectra from HCl and HBr, respectively. In order to assign the spectrum one has to consider overlapping lines and intermediate coupling. The bars in the lower part indicate the two separate spectra arising from the spin-orbit splitting of the I 4d core hole state.

accompanying line 5 is consequently assigned to the $4d_{3/2}$ $(v=0) \rightarrow \pi^{-2}\,{}^1\Delta_2$ $(v=1)$ transition. This assignment implies that the $v=1$ component has approximately the same intensity as the $v=0$ component. (It should be noted that to obtain the correct intensities a sloping background has to be subtracted.) This agrees with the strong $v=1$ components observed in the corresponding transition in HCl and HBr. The $v=2$ component is hidden under the flank of line 6.

From the observed spin-orbit splitting of the I 4d components of 1.76 eV (cf figure 1) we expect that the $4d_{5/2}$ $(v=0) \rightarrow \pi^{-2}\,{}^3\Sigma_1^-$ $(v=0)$ transition falls under line 7 in the third group of lines. In table 2 we have listed the double ionisation energies, i.e. the 4d binding energies minus the measured Auger energies. Line 6 has a weak counterpart in the $\frac{3}{2}$ spectrum in line 1. If line 6 were explained by the $4d_{5/2}$ $(v=1) \rightarrow \pi^{-2}\,{}^3\Sigma_1^-$ $(v=0)$ transition the intensity would be unusually high and it would be difficult to understand why its counterpart line 1 is so weak. Instead we suggest that line 6 corresponds to the $4d_{5/2}$ $(v=0) \rightarrow \pi^{-2}\,{}^3\Sigma_0^-$ $(v=0)$ transition. This assignment implies a splitting between the two multiplet components of the ${}^3\Sigma^-$ state of 220 meV. This is the splitting expected from a comparison with the Xe NOO spectrum (Werme *et al* 1972) where the splitting between the ${}^3P_0$ and ${}^3P_1$ components is observed to be 0.22 eV. It is also interesting to notice that the ${}^3P_0$ component is not observed at all in the

Table 1. NVV Auger electron energies in HI.

Line no	Kinetic energy (eV)	Assignment
1	29.990	$4d_{3/2}(v=1) \rightarrow \pi^{-2}\,{}^3\Sigma_1^-(v=0)$
2	29.770	$4d_{3/2}(v=0) \rightarrow \pi^{-2}\,{}^3\Sigma_1^-(v=0)$
3	29.550	$4d_{3/2}(v=0) \rightarrow \pi^{-2}\,{}^3\Sigma_1^-(v=1)$
4	28.970	$4d_{3/2}(v=0) \rightarrow \pi^{-2}\,{}^1\Delta_2(v=0)$
5	28.730	$4d_{3/2}(v=0) \rightarrow \pi^{-2}\,{}^1\Delta_2(v=1)$
6	28.200	$4d_{5/2}(v=0) \rightarrow \pi^{-2}\,{}^3\Sigma_0^-(v=0)$
7	28.010	$4d_{5/2}(v=0) \rightarrow \pi^{-2}\,{}^3\Sigma_1^-(v=0)$
8	27.730	$4d_{5/2}(v=0) \rightarrow \pi^{-2}\,{}^3\Sigma_1^-(v=1)$
9	27.480	$4d_{3/2}(v=0) \rightarrow \pi^{-2}\,{}^1\Sigma_0^+(v=0)$
10	27.290	$4d_{3/2}(v=0) \rightarrow \pi^{-2}\,{}^1\Sigma_0^+(v=1)$
11	27.150	$4d_{5/2}(v=0) \rightarrow \pi^{-2}\,{}^1\Delta_2(v=0)$
12	26.970	$4d_{5/2}(v=0) \rightarrow \pi^{-2}\,{}^1\Delta_2(v=1)$
13	25.870	
14	25.730	$4d_{5/2}(v=0) \rightarrow \pi^{-2}\,{}^1\Sigma_0^+(v=0)$
15	25.550	$4d_{5/2}(v=0) \rightarrow \pi^{-2}\,{}^1\Sigma_0^+(v=1)$
16	25.390	$4d_{5/2}(v=0) \rightarrow \pi^{-2}\,{}^1\Sigma_0^+(v=2)$

Table 2. HI double ionisation energies (eV)

Line no	Relative to $4d_{5/2}$	Relative to $4d_{3/2}$	Vibronic states
1		29.260	$\pi^{-2}\,{}^3\Sigma_0^-(v=0)$
2		29.480	$\pi^{-2}\,{}^3\Sigma_1^-(v=0)$
3		29.700	$\pi^{-2}\,{}^3\Sigma_1^-(v=1)$
4		30.280	$\pi^{-2}\,{}^1\Delta_2(v=0)$
5		30.520	$\pi^{-2}\,{}^1\Delta_2(v=1)$
6	29.290		$\pi^{-2}\,{}^3\Sigma_0^-(v=0)$
7	29.480		$\pi^{-2}\,{}^3\Sigma_1^-(v=0)$
8	29.760		$\pi^{-2}\,{}^3\Sigma_1^-(v=1)$
9		31.700	$\pi^{-2}\,{}^1\Sigma_0^+(v=0)$
10		31.960	$\pi^{-2}\,{}^1\Sigma_0^+(v=1)$
11	30.340		$\pi^{-2}\,{}^1\Delta_2(v=0)$
12	30.520		$\pi^{-2}\,{}^1\Delta_2(v=1)$
13	31.620		
14	31.760		$\pi^{-2}\,{}^1\Sigma_0^+(v=0)$
15	31.940		$\pi^{-2}\,{}^1\Sigma_0^+(v=1)$
16	32.100		$\pi^{-2}\,{}^1\Sigma_0^+(v=2)$

N_4OO spectrum while in the N_5OO spectrum this component is more intense than the $^3P_1$ component. With the assignment made here the HI NVV Auger spectrum qualitatively exhibits the same intensity relations as the NOO Auger spectrum from atomic Xe. It should, however, be noticed that line 1 gets intensity from both the $4d_{3/2}$ $(v=1) \rightarrow \pi^{-2}\,{}^3\Sigma_1^-$ $(v=0)$ transition and the $4d_{3/2}$ $(v=0) \rightarrow \pi^{-2}\,{}^3\Sigma_0^-$ $(v=0)$ transition. At present it is difficult to say which process gives the largest contribution to the intensity of this line.

The assignments of the second group of lines to the $\pi^{-2}\,{}^1\Delta_2$ final state and the third group to the $\pi^{-2}\,{}^3\Sigma^-$ final state are also supported by considering the relative

position of the corresponding lines in the HCl and HBr Auger electron spectra. It is seen that with increasing atomic number these two groups are shifted with respect to each other in a regular way.

The fourth group of lines 8–12 is complicated to assign due to the overlapping of lines. It is therefore favourable to first discuss the fifth group of lines, 13–16, where the assignment is more obvious. With the assignments made above for the $^3\Sigma$ and $^1\Delta$ states the main explanation for the lines 14–16 is in terms of the $4d_{5/2} \rightarrow \pi^{-2}\,{}^1\Sigma_0^+$ transition. These lines seem to correspond to a vibrational progression. We therefore associate the lines 14, 15 and 16 with the $4d_{5/2}\,(v=0) \rightarrow \pi^{-2}\,{}^1\Sigma_0^+\,(v=0, 1, 2)$ transitions, respectively. Line 13 is more difficult to explain. Obviously it gets intensity from the $4d_{5/2}\,(v=1) \rightarrow \pi^{-2}\,{}^1\Sigma_0^+\,(v=0)$ transition, but the intensity of line 13 seems to be larger than expected for such a transition. The intensity of the whole fifth group of lines seems to be larger than expected from the other groups of lines. One might speculate if, e.g., a transition to a $\sigma^{-1}\pi^{-1}$ configuration could be hidden under this group of lines and in particular contribute to the intensity of line 13. However, at the moment we have no calculations to verify this. It should be noted that such states also overlap in the cases of HCl and HBr and are expected to be dissociative, thus giving rise to broad lines.

When the assignment of the fifth group of lines is made it is a simple matter to identify lines 8–12 from the known spin-orbit splitting of the I 4d components. Obviously line 8 gets intensity from the $4d_{5/2}\,(v=0) \rightarrow \pi^{-2}\,{}^3\Sigma_1^-\,(v=1)$ transition, however it also coincides with a $4d_{3/2}\,(v=1) \rightarrow \pi^{-2}\,{}^1\Sigma_0^+\,(v=0)$ transition. Lines 9 and 10 are due to the high-energy counterparts to lines 14 and 15. Line 12 is unambigously associated with the $4d_{5/2}\,(v=0) \rightarrow \pi^{-2}\,{}^1\Delta_2\,(v=1)$ transition. Line 11 does not fit exactly to the $4d_{5/2}\,(v=0) \rightarrow \pi^{-2}\,{}^1\Delta_2\,(v=0)$ transition but this is probably due to an overlap between lines 10 and 11.

All the assignments made above are summarised in tables 1 and 2.

3.3. Equilibrium geometries and potential curves for the π^{-2} states in HI^{2+}

In the case of the Auger spectra of HCl and HBr it was possible to make a comparatively good estimate of the relative intensities of the vibrational components in the spectra and make a reasonable sketch of the potential curves for the dicationic states. From figure 2 it is seen that, due to the overlap between the peaks and to the high background it is only possible to make a more qualitative analysis. The vibrational energies and relative intensities that are obtained are summarised in table 3. Using the harmonic approximation we have calculated Franck-Condon factors for the Auger transitions to the $\pi^{-2}\,{}^3\Sigma_1^-$, $\pi^{-2}\,{}^1\Delta_2$ and $\pi^{-2}\,{}^1\Sigma_0^+$ final states in order to obtain an estimate of the corresponding equilibrium internuclear distances. In this simulation we have used the I 4d core-hole state geometry that has been obtained above, i.e. we have also considered the contribution to the spectra from the $v=1 \rightarrow v=v'$ transitions. The resulting equilibrium distances are shown in table 4 together with the binding energies of the states. In contrast to the findings for HCl^{2+} and HBr^{2+} the equilibrium bond distance for the $^1\Sigma_0^+$ state is smaller than for the $^1\Delta_2$ state. This could be due to the experimental uncertainty in the present results. It is also possible that the geometry is influenced by the interaction between the states with $\Omega=0$, i.e. between the $^1\Sigma_0^+$ and the $^3\Sigma_0^-$ states.

In order to draw the potential curves, as we have done previously for the corresponding states in HCl and HBr, it is necessary to estimate the dissociation energy for a suitable Morse potential. Since no anharmonicity can be inferred from any of the

Table 3. Relative energies and intensities for the vibrational states in some of the $N_{4,5} \rightarrow (\pi^{-2})$ Auger electron bands in HI.

Transition	Vibrational quantum no of the final state	Relative energy (meV)	Relative intensity
$4d_{3/2}(v=0) \rightarrow \pi^{-2}\,{}^3\Sigma_1^-$	0	0	1
	1	220	≃0.2
$4d_{3/2}(v=0) \rightarrow \pi^{-2}\,{}^1\Delta_2$	0	0	1
	1	220	≃1
$4d_{5/2}(v=0) \rightarrow \pi^{-2}\,{}^1\Sigma_0^+$	0	0	1
	1	160	≃0.5
	2	320	≃0.1

Table 4. Adiabatic binding energies and equilibrium internuclear distances for π^{-2} doubly ionised states.

State	Adiabatic binding energy (eV)	Internuclear distance (Å)
$^3\Sigma_0^-$	29.29 (5)	—
$^3\Sigma_1^-$	29.48 (5)	1.87 (6)
$^1\Delta_2$	30.28 (5)	1.92 (6)
$^1\Sigma_0^+$	31.77 (5)	1.88 (6)

states we have tentatively used the dissociation energy of the ground state. This energy of 3 eV is to be considered as an upper limit. At large internuclear distances the doubly ionised states dissociate via the Coulomb explosion mechanism into I^+ and H^+. The $^3\Sigma_1^-$ state dissociates into the $I^+(^3P)+H^+$ state whereas the $^1\Delta_2$ and $^1\Sigma_0^+$ states dissociate into the $I^+(^1D)+H^+$ state of the free ions. Using the known atomic energies for these states it is possible to sketch a Coulomb potential for large internuclear distances. The resulting potential curves are shown in figure 3. It should be noticed that, since only an upper limit for the dissociation energy could be used, the curves are tentatively sketched over quite a large range of internuclear distances near the crossing point between the Morse curve and the Coulomb potential curve.

Acknowledgment

The authors would like to thank Professor U Gelius for strong support and J-O Forsell and Lennart Eriksson for assistance with the experimental work. This work has been supported by the Swedish Natural Science Research Council. One of us, NC, thanks CAPES in Brazil for financial support.

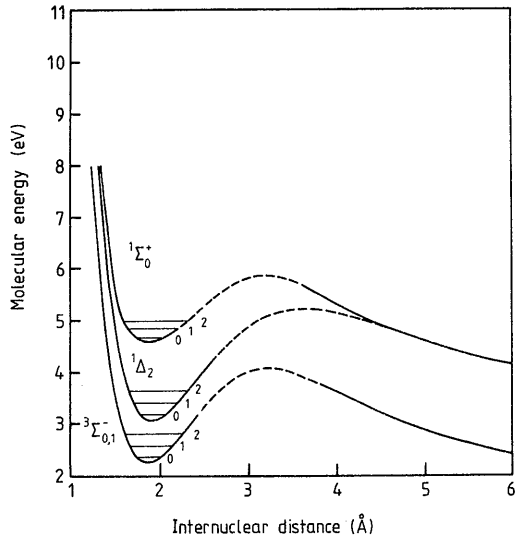

Figure 3. Potential curves for doubly ionised states in HI belonging to the π^{-2} configuration. The molecular energy is relative to the I^+ and H^+ ground state. In the vicinity of the equilibrium internuclear distance a Morse curve is used and for large internuclear distances a Coulomb curve is used. In a rather large region near the intersection point of these curves the potential is tentative and has therefore been drawn as a broken curve. See text.

References

Baltzer P, Carlsson-Göthe M and Wannberg B 1988a *Institute of Physics Report* Uppsala University UUIP-1182

Baltzer P, Wannberg B, Svensson S and Karlsson L 1988b *Institute of Physics Report* Uppsala University UUIP-1190

Huber K P and Herzberg G 1979 *Constants of Diatomic Molecules* (New York: Van Nostrand-Reinhold)

Karlsson L, Baltzer P, Svensson S and Wannberg B 1988 *Phys Rev. Lett.* **60** 2473

Keski-Rahkonen O and Krause M O 1974 *At. Data Nucl. Data Tables* **14** 139

Morin P and Nenner I 1987 *Phys. Scr.* T **17** 171

Svensson S, Karlsson L, Baltzer P, Keane M P and Wannberg B 1989 *Phys. Rev.* A to be published

Wannberg B, Svensson S, Keane M P, Karlsson L and Baltzer P 1989 *Chem. Phys.* **133** 281

Werme L O, Bergmark T and Siegbahn K 1972 *Phys. Scr.* **6** 141